Photo-Responsive Water Filtration Membranes Based on Polymerizable Columnar Liquid Crystals with Azo Moieties

Document status and date:
Published: 04/07/2022

Document Version:
Publisher's PDF, also known as Version of Record (includes final page, issue and volume numbers)

Please check the document version of this publication:

• A submitted manuscript is the version of the article upon submission and before peer-review. There can be important differences between the submitted version and the official published version of record. People interested in the research are advised to contact the author for the final version of the publication, or visit the DOI to the publisher's website.
• The final author version and the galley proof are versions of the publication after peer review.
• The final published version features the final layout of the paper including the volume, issue and page numbers.

Link to publication

Photo-Responsive Water Filtration Membranes Based on Polymerizable Columnar Liquid Crystals with Azo Moieties

Patricia P. Marín San Román and Rint P. Sijbesma

New materials developed in the last years promise to contribute significantly to the preparation of membranes with improved performance in water filtration. Specifically, the use of dynamic-responsive systems provides reversibility of the membrane properties. In this work, a reversible photo-switchable membrane based on templated liquid crystals is presented. Crosslinking of a columnar network, formed by the self-assembly of a discotic supramolecular complex with a photo-responsive moiety, results in a switchable filtration membrane. The azo groups in the membrane undergo a photoinduced *trans-cis* isomerization by irradiation with 365 nm light and relax back to the *cis* isomer with a lifetime of 5.7 h or within a few minutes by irradiation at 455 nm. The membranes have a light-induced reversible change in the water permeability and molecular weight cut off of poly (ethylene glycol). The effective pore size of the *trans* isomer (1.2 nm) increases to 1.4 nm for the *cis* isomer. Rejection of the organic dye Rhodamine B is reversibly switched between 50 and 85% by alternating irradiation at 365 nm and 455 nm. The reversible and specific switching demonstrates the potential of this system for light-controlled separation in nanoporous membranes.

1. Introduction

Smart materials are of increasing importance due to their ability to change properties under the influence of external stimuli.[1] The use of light, a versatile stimulus that can be applied remotely, rapidly, and with high spatial resolution, has proven to be a clean and nondestructive manner to switch molecules between different states.[2] Recently the incorporation of light-responsive materials has been exploited with significant benefits in many fields including drug delivery, sensing, robotics, microfluidics, data storage, and water treatment.[3,4]

The approach used to obtain these smart materials is based on the incorporation of photo-switchable molecular moieties

in the material, that isomerize reversibly upon irradiation at specific wavelengths, leading to on-demand changes in material properties. For instance, in light-responsive azobenzenes, reversible *cis-trans* isomerization via irradiation and thermal relaxation gives changes in geometry, polarity, and electrical properties.[5,6] Due to the stability, versatility, and robustness of these chromophores, azobenzenes have been included as photo-responsive moieties in materials where light produces a modification of properties such as wettability, binding, shape, color, and alignment.[7] Light-induced changes in polymers allow their application as molecular actuators for soft-robotics,[8] uptake and release of guests for drug delivery systems[9,10] or for biomimetic modification of surface properties,[11] among others.[12]

A strongly growing interest in sustainability and reducing energy consumption has increased the need for efficient separation of molecular mixtures. The integration of molecular photo-switches in membranes is a promising way to control separation processes with such a versatile stimulus as light.[13] The photo-induced changes in pore size and polarity in nanoporous materials permit a change in size-selective absorption.[14–17] Therefore, photo-responsive membranes can be used to control the permeation and molecular separation in gas and liquid mixtures.[18,19] It is possible to obtain these membranes either by incorporation of molecular photo-switches during their synthesis, or by grafting photo-responsive polymers on the membrane surface after their preparation. As an example of the first strategy, molecular recognition materials with photo-switchable properties have been made by molecular imprinting, allowing specific binding interactions with target molecules.[20] The grafting strategy, on the other hand, has been used to tune wettability and other surface properties to create self-cleaning or antifouling membranes.[21]

A number of light-responsive filtration membranes have been reported in which the transport of solutes through the pores is tuned with irradiation.[22–26] The pores in a photo-switchable membrane can also act as photo-responsive valves allowing the regulated transport of molecules. Gating channels that reversibly open and close have been successfully developed using polyelectrolyte and inorganic nanoporous membranes containing azo moieties.[27–30] However, photo-switching has not been used as a dynamic process that permits control over the passage of solutes in water filtration membranes yet.

P. P. Marín San Román, R. P. Sijbesma
Supramolecular Polymer Chemistry Group
Department of Chemical Engineering & Chemistry and Institute for Complex Molecular Systems
Eindhoven University of Technology
Eindhoven, The Netherlands
E-mail: r.p.sijbesma@tue.nl

The ORCID identification number(s) for the author(s) of this article can be found under https://doi.org/10.1002/admi.202200341.

ADVANCED
SCIENCE NEWS
www.advancedsciencenews.com

ADVANCED
MATERIALS
INTERFACES
www.advmatinterfaces.de
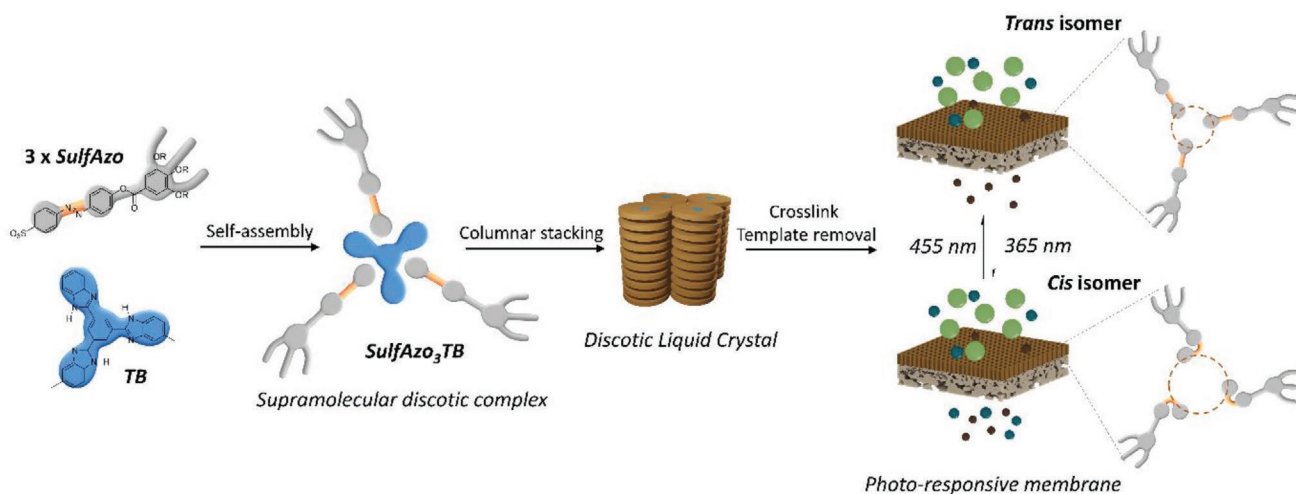
Figure 1. Schematic representation of the photo-switchable supramolecular complex formation, which forms a columnar mesophase that is transferred into support and crosslinked with UV light. The *trans-cis* isomerization of azo moieties with UV light in the filtration membrane changes the permeability of solutes.

Recently, our group has developed new supported membranes for water filtration based on supramolecular liquid crystal with charge and size selectivity in the rejection of organic molecules and ions.[31] A templated supramolecular system, similar to that developed by the group of Kim for the fabrication of porous materials,[32] was used by us as the selective layer of a filtration membrane. The formation of pores occurs after crosslinking of a columnar network and removal of a template molecule, a strategy that has previously been applied for the study of pore alignment and size and charge selectivity of self-standing nanoporous films in absorption.[33–35] Moreover, the photo-switchable properties of porous films of a similar templated system containing azo moieties have also been demonstrated.[17] The application of this approach to the fabrication of membranes with light-controlled selectivity would be a valuable next step in the development of responsive filtration membranes.

Herein, the development of a photo-responsive filtration membrane based on a new supramolecular columnar liquid crystal SulfAzo₃TB is reported. The photo-induced isomerization of the azo compound is studied in solution and in the crosslinked network. In supported membranes, photoisomerization is found to lead to stable, yet reversible changes in permeability that last for several hours and control the selectivity towards small organic molecules in the membrane with light (**Figure 1**).

2. Results and Discussion

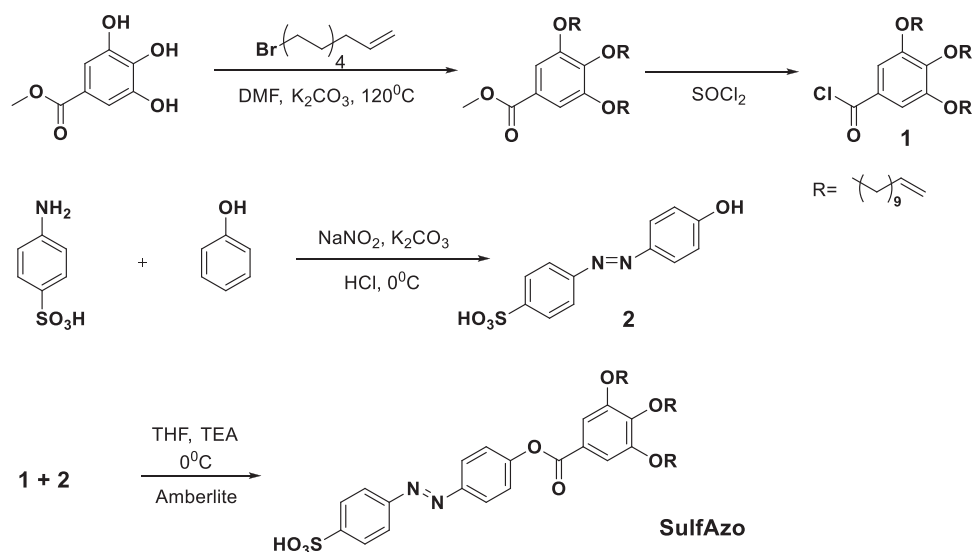### 2.1. Design and Characterization of SulfAzo Wedge-Shaped Monomer

The supramolecular complex SulfAzo₃TB is composed of two components: a tris-benzimidazolyl benzene core molecule (TB), that acts as the template, and the wedge-shaped monomer SulfAzo containing an azo moiety and double bonds in the alkyl chains for later crosslinking. These molecules were synthesized separately: TB was synthesized as previously reported[36] and SulfAzo was prepared following a three-step synthetic route shown (**Scheme 1**).

Acid chloride derivative **1** was obtained from the alkylation of the hydroxyl groups of methyl gallate with 11-bromo-1-undecene followed by chlorination of the tris-alkene ester. The diazonium salt for diazo coupling was prepared by the diazotization of p-aminobenzene sulfonate with sodium nitrite. Subsequently, this salt was reacted with phenol to yield azo product **2** as an orange powder after precipitation and drying under vacuum, and the molecular structure was verified by NMR (Figures S1 and S2, Supporting Information). Finally, compounds **1** and **2** reacted in tetrahydrofuran and triethylamine to give the salt of SulfAzo. After ion-exchange on Amberlite IR 120 (acidic form) the photo-switchable sulfonic acid (SulfAzo) was obtained pure as confirmed with ¹H-NMR and ¹³C-NMR (Figures S3 and S4, Supporting Information).

SulfAzo is liquid crystalline at room temperature (Figure S5, Supporting Information) and X-ray diffraction (XRD) studies showed the formation of a columnar rectangular mesophase at room temperature after annealing with lattice parameters $a = 6.34$ nm and $b = 12.92$ nm (Figure S6 and Table S1, Supporting Information), following the trend reported for similar compounds.[37,38]

2.2. Formation of SulfAzo₃TB Complex

A mixture of TB with 3.2 equiv. of SulfAzo afforded an H-bonded 1:3 complex (**Figure 2**a) as is evident from a new band at 3250 cm⁻¹ in the FT-IR spectrum (Figure 2b), which corresponds to the imidazolium N⁺-H stretching vibration.[34] The addition of a small excess (3.2 instead of 3 equiv.) of SulfAzo prevented phase separation of crystalline TB. The observation of the complex under polarizing optical microscopy (POM) at room temperature showed a mosaic-like shaped texture typical for columnar mesophases (Figure 2c). XRD data showed the formation of a columnar rectangular mesophase after annealing at 80 °C with lattice parameters $a = 4.79$ nm and $b = 5.32$ nm (Figure S8a and Table S2, Supporting Information). The formation of columnar nanostructures from the self-assembly of compounds similar to SulfAzo with ionic templates has been shown in the literature.[39]

ADVANCED
SCIENCE NEWS
www.advancedsciencenews.com

ADVANCED
MATERIALS
INTERFACES
www.advmatinterfaces.de

Scheme 1. Synthesis of wedge-shaped azo derivative SulfAzo.

2.3. Fabrication of Nanoporous Films

Nanoporous polymer films were obtained from the columnar mesophase of the complex using the photochemical thiol-ene click reaction as crosslinking method (**Figure 3**a).[40] The obtained dry films (thickness 0.5–1 µm) (Figure 3b) showed a texture in POM with small conic focal domains corresponding to a columnar mesophase (Figure 3c). The disappearance of the C=C bending band at 907 cm^{-1} in the FT-IR spectrum indicated almost full conversion of the alkene groups (Figure 3d).[41] Finally, the films were immersed and shaken in dimethyl sulfoxide to remove the template, which is confirmed with the full disappearance of the N^+-H stretching band at 3250 cm^{-1} in Figure 3d.
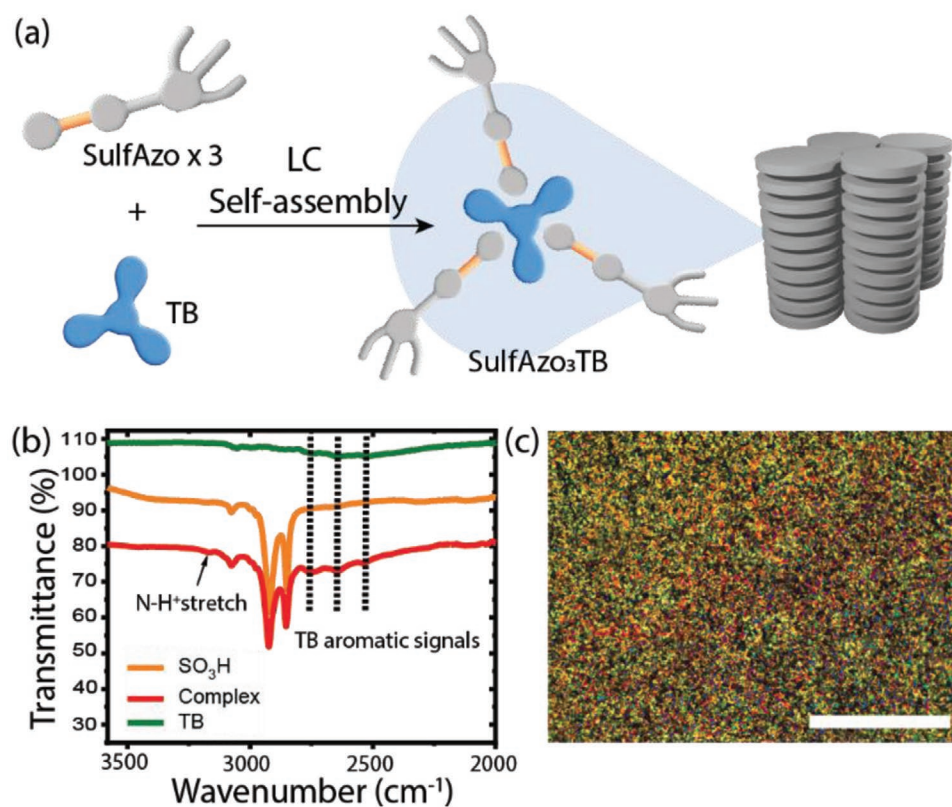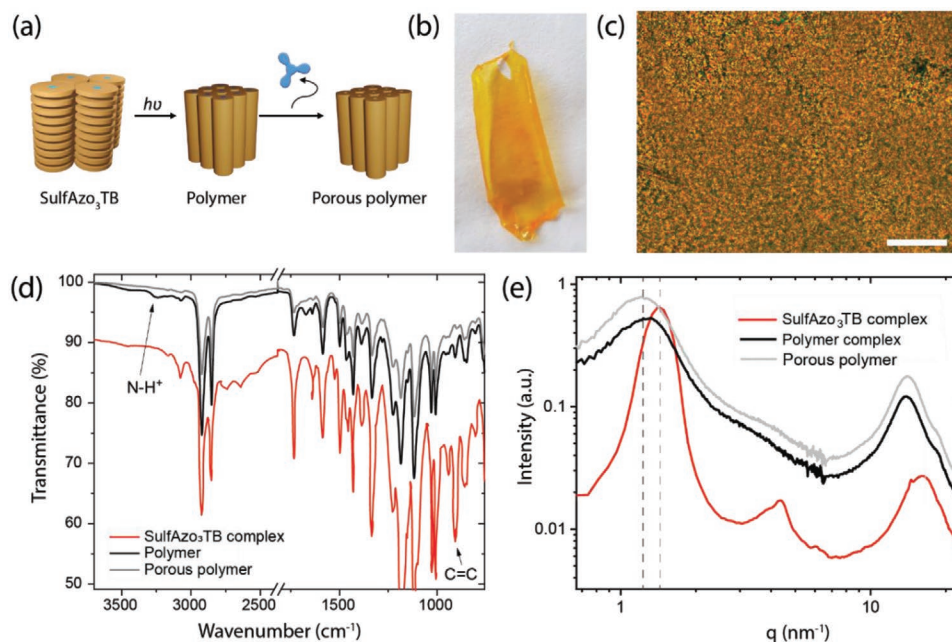

Figure 2. a) Formation of the supramolecular discotic complex SulfAzo₃TB via H-bonding. b) IR spectra of SulfAzo, TB, and the 3:1 mixture indicating the formation of an H-bonded complex. c) Cross-polarized light micrograph of a 3.2:1 mixture of SulfAzo and TB at room temperature with a scale bar of 50 µm.

Figure 3. a) Crosslinking of the CLC and consecutive removal of the TB template molecule. b) Sample of the polymer film. c) POM picture of the film. Scale bar is 50 µm. d) FT-IR spectra comparing SulfAzo₃TB before and after polymerization where the = C–H stretching band of the double bond C=C disappeared. After removing the template, the peak corresponding to N–H⁺ from TB disappeared. e) 1D Wide-angle X-ray diffractograms of the polymerization mixture (red), after polymerization (black), and after template removal (grey).

WAXS studies were carried out to check the retention of the columnar order after crosslinking and removal of the template (Figure 3e). Polymerization affected the columnar order, and the first maximum peak shifted from 1.42 to 1.29 nm⁻¹, indicating a 10% decrease in periodicity, meaning larger distance due to the addition of the crosslinker. When the TB template was removed, the q-value of the first maximum decreased further to 1.24 nm⁻¹. A reflection from the inter-disk distance at wide angles is visible as a shoulder at d = 0.34 nm for the polymerized material, indicating some order in the stacking of the columns.

2.4. Photo-Isomerization of the Monomer in Solution and of the Crosslinked Nanoporous Films

Photo-isomerization of the azo group is responsible for inducing changes in the pores. Isomerization was studied in the monomer as well as in the thin film as their photophysical properties can be different.[17] The UV-Vis spectrum of a 100 µM chloroform solution of SulfAzo showed an intense $\pi \rightarrow \pi^*$ absorption band at 325 nm corresponding to the *trans* isomer and a much weaker n → π^* band at 465 nm (red curve, **Figure 4**).[42] Upon irradiation of the solution with 365 nm UV
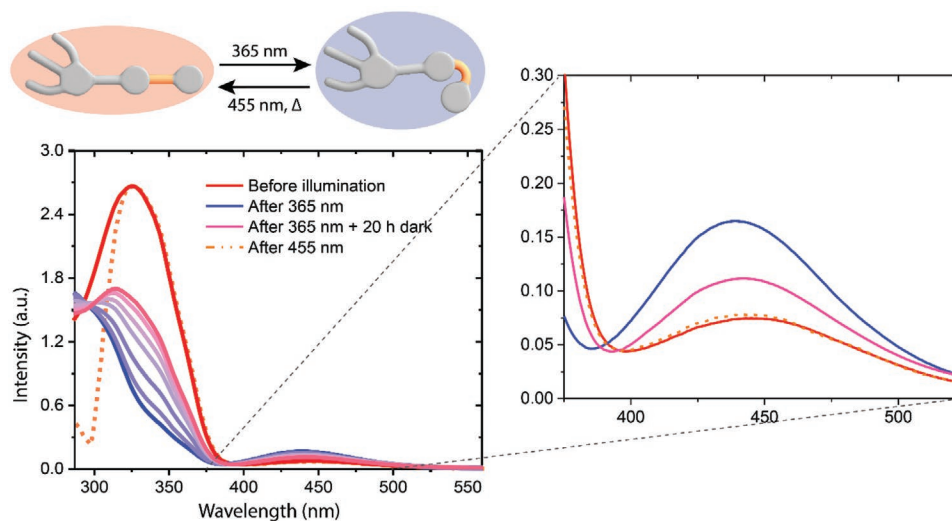
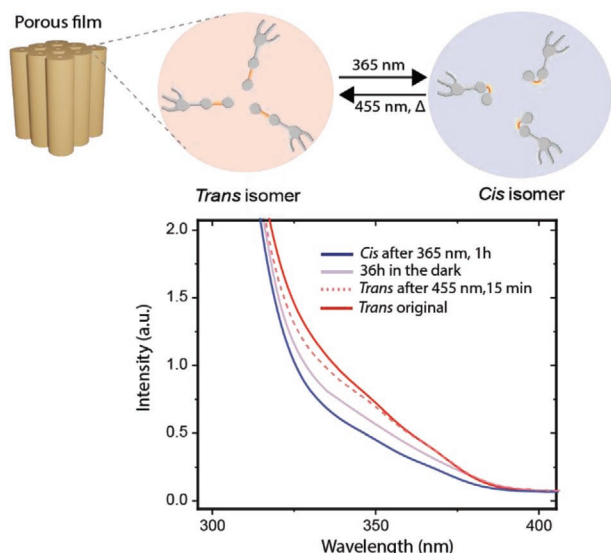**Figure 4.** UV-Vis spectra of SulfAzo in CHCl₃ (100 µm) after 365 nm light irradiation for 15 min, after thermal relaxation up to 20 h, and after 455 nm irradiation for 15 min (dashed line) and zoom-in on the right of the band at 455 nm.

light, the intensity of the $\pi - \pi^*$ transition band at 325 nm decreased strongly, indicating *trans* to *cis* isomerization. After 15 min, a photo-stationary state was reached (blue curve, Figure 4) with the decrease of the 325 nm absorption band and a slight increase at 440 nm as the result of *trans*-to-*cis* photo-isomerization. The sample was let relax back in the dark, showing an increase of the 325 nm band and a decrease at 455 nm, but as shown in Figure 4, total conversion was not reached, and only 52% of the population of the *trans* isomer was recovered after 20 h. Additional experiments on the same solution showed that partial isomerization is reproducible (see Figure S10, Supporting Information) and fitting of the repeated thermal *cis-trans* isomerization experiments suggests that full conversion to the transform is not attained under thermal conditions. The reason for the incomplete thermal *cis-trans* isomerization is not known. This suggests that longer times are needed for the full recovery of the *trans* isomer. However, by irradiation of the solution with 455 nm blue light, the process was accelerated, reaching complete recovery of the *trans* population in only 15 min (dashed line Figure 4).

In order to study both states of a photo-switchable membrane, the lifetime of each *trans* and *cis* isomers must be sufficient. Therefore, the thermal relaxation of the azobenzene was investigated for SulfAzo to obtain the lifetime of the *cis* isomer. By monitoring the change in absorption at 325 nm, the lifetime of the *cis* isomer was calculated. The data was fitted with an exponential model, yielding a lifetime for the *cis* isomer of 7.1 h at room temperature (Figure S9, Supporting Information).[17] The observed reversibility of the isomerization process and the lifetime value obtained are in line with similar azo compounds reported by our group.[17]

The photo-switching characteristics were also studied in thin films (thickness ≈0.5 µm) of the porous polymer with SulfAzo$_3$TB complex (**Figure 5**), revealing a similar behavior as SulfAzo in solution. Upon irradiation at 365 nm, the inten-

sity of the band at 325 nm decreased to *cis* in 1 h, a bit longer than in solution due to restricted movement in the crosslinked network. When the *cis*-enriched film was allowed to relax back thermally at room temperature in the dark, the initial *trans* state was not reached even for long times (after 36 h there is still 50% of *cis* isomer present). The thermal relaxation data was plotted and fitted with an exponential model in the same way as for the monomer in solution, showing a lifetime of 5.7 h (Figure S11, Supporting Information). *Cis-trans* isomerization was complete after only 15 min when the film was irradiated with 455 nm light.

The slightly shorter lifetime of the *cis* isomer in the polymer compared to in solution is related to a restriction of the molecular movement in the solid-state, as was observed in similar networks.[17,43,44] To achieve full conversion to the *trans* isomer, blue light (455 nm) was used as a stimulus.

As a result of these observations, the lifetime of each state was sufficient to study the filtration properties in supported membranes in the pure *trans* and the *cis* enriched films separately.

XRD measurements of the films were performed to study whether the photoisomerization process affected the morphology of the network at room temperature. In Figure S11, Supporting Information the WAXS pattern of the nanoporous film before and after irradiation at 365 nm is shown. An increase of the lattice parameter (lower q-value for the first diffraction peak) was observed after photoisomerization to the *cis* isomer (from $a = 5.07$ nm to 6.22 nm). When the film was irradiated with 455 nm light to go back to the *trans* isomer, the initial lattice spacing was almost recovered (a *trans* back = 5.19 nm). These results confirm that the reversibility of the isomerization process translates to a reversible change of the nanostructure with light irradiation.

2.5. Membrane Formation and Characterization

Thin film supported membranes are normally used for nanofiltration purposes. In order to get good filtration performance with high fluxes, a very thin active layer is needed which requires the use of porous support to give mechanical strength. Therefore, supported nanofiltration membranes were fabricated by following a published procedure[31] as shown in **Figure 6**a. The procedure consists of 3 steps: 1) spin coating a thin layer of the mixture of LC, crosslinker, and photo-initiator in CH$_3$Cl:EtOH (8:2) on PVA-coated glass; 2) transferring the layer to a PES support by heating and pressing, and 3) fixating the active layer by irradiation with UV light for 10 min. High-resolution scanning electron microscopy showed an average thickness of the active layer of approximately 300 nm on top of a porous PES support layer of around 300 µm thickness (Figure 6b).

Figure 5. UV-Vis spectra of SulfAzo$_3$TB films of irradiation at 365 nm for 1 hour to reach the *cis* isomer, thermal relaxation for 36 h without reaching total conversion to *trans* isomer, and after 15 min of 455 nm with a total recovery of the *trans* population.

### 2.5.1. Effect of Photo-Switching on Filtration Properties

The long lifetime of 5.7 h for the *cis* isomer in solid-state makes it possible to study filtration in these isomeric states of the membrane, while completing isomerization back to the *trans* isomer
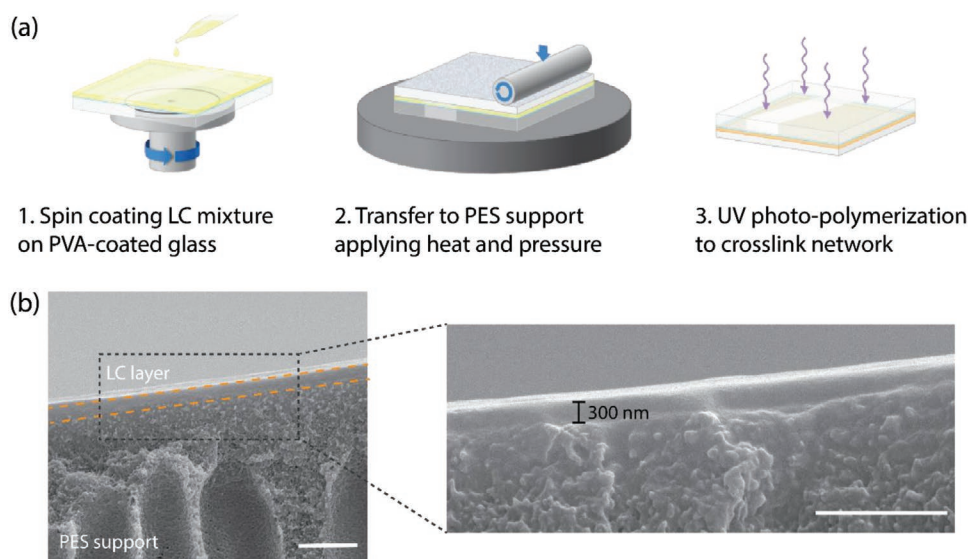
Figure 6. a) Membrane fabrication process where the LC solution is spin-coated and later transferred to a PES support and b) Zoom out and zoom in HR-SEM images showing a perfectly defined and attached 300 nm active layer on top of the support with scale bars of 1 μm and 500 nm respectively.

by irradiation at 455 nm allows for repeated switching between states. To verify the photo-responsiveness of the membrane, filtration tests were performed before and after irradiation with 365 and 455 nm light as represented in **Figure 7**a (Real set-up in Figure S13, Supporting Information). The membrane was irradiated inside the filtration cell alternatingly with 365 and
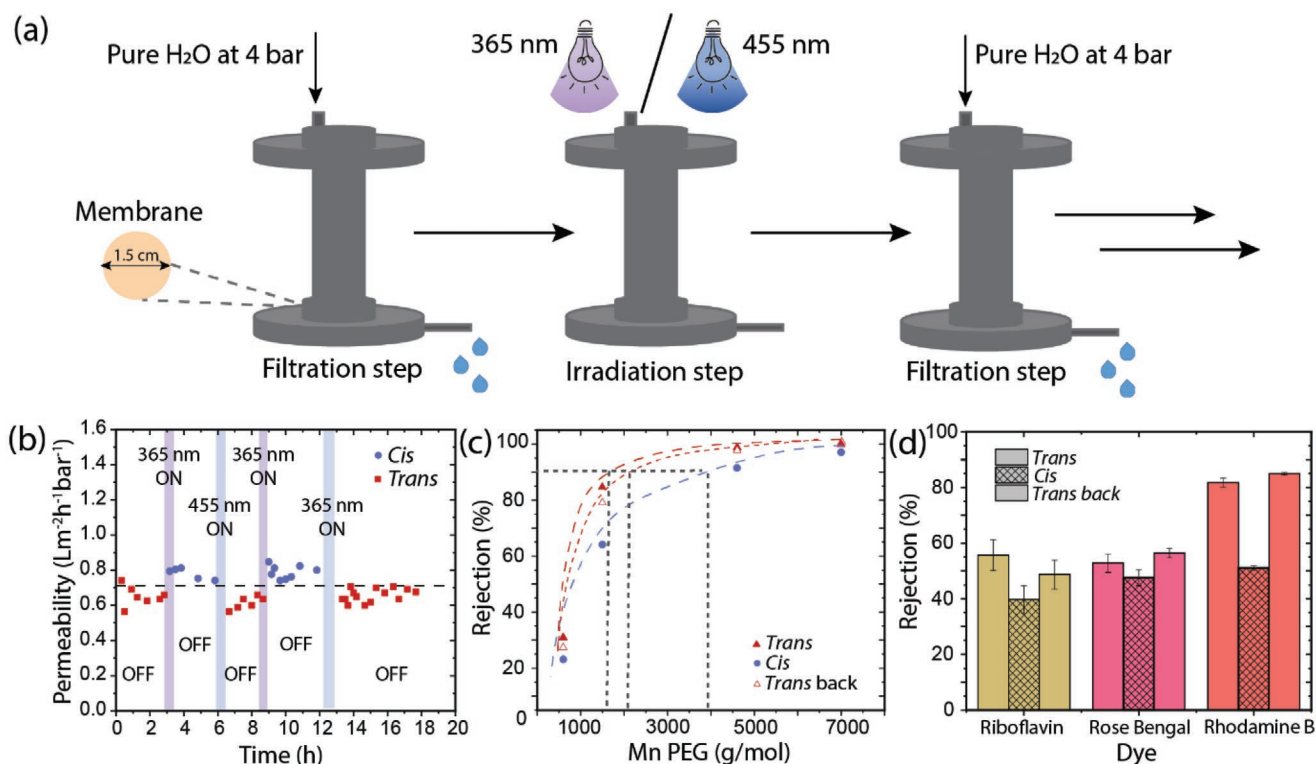
Figure 7. a) Filtration experiments with a supported membrane of SulfAzo₃TB on PES. Schematic illustration of the filtration process with irradiation steps to switch isomeric state in the membrane. b) Plot of pure water permeability as a function of time with alternating UV (365 nm) and blue (455 nm) light irradiation. c) MWCO curves for the membrane in the initial *trans* state (red filled triangles), after 1 h of 365 nm irradiation in *cis* state (blue circles) and after 15 min of 455 nm in *trans* state back (red open triangles). d) Plot of dye rejection before and after irradiation at 365 nm, and after relaxation back to *trans* with 455 nm light. The values of permeability and rejection are based on three permeate samples of three different membranes.

**ADVANCED
SCIENCE NEWS**

www.advancedsciencenews.com

**ADVANCED
MATERIALS
INTERFACES**

www.advmatinterfaces.de

455 nm light for 1 h and 15 min respectively. The flux of pure water was measured over time for the different states of the membrane for three cycles (Figure 7b). A reproducible and stable pattern of higher and lower values of water flux (0.78 ± 0.004 and 0.64 ± 0.019 L m^{-2}h^{-1}bar^{-1}) was observed for *cis* and *trans* states respectively, confirming that the flux is dependent on the state of the polymer and that the state can be reverted by irradiation with a specific wavelength.

The molecular weight cut-off (MWCO) of the membrane, which is the molecular weight at which 90% of a solute is rejected, was determined in both isomeric states. Filtration tests of a mixture of four PEGs with an Mn ranging from 600 to 7000 g mol^{-1} was performed with membranes in the *cis* and the *trans* state. The PEG rejection curves for the membrane before and after irradiation at 365 nm (*trans* followed by *cis*) and after irradiation with 455 nm light (back to *trans*) are represented in Figure 7c. At a specific PEG molecular weight, a higher retention was always obtained for the membrane in the *trans* state indicating a smaller pore size. In line with this, a higher MWCO and a lower rejection over the full MWCO range were observed for the *cis* state (≈4000 g mol^{-1}) compared to the *trans* state (≈2000 g mol^{-1}), which is in full agreement with the higher permeability for the *cis* membrane as shown in Figure 7b. Additionally, after the relaxation back to the *trans* state, a lower MWCO value was obtained again, very close to the initial value of the rejection curve in the *trans* state and confirming the reversibility of the process. These observations are in line with the hypothesized changes in pore size due to the opening of the structure after isomerization from *trans* to *cis*. Based on the MWCO values, pore sizes of 1.2 and 1.6 nm, respectively are calculated for the *trans* and *cis* membranes, respectively.

The effect of the isomeric state of the membrane on the rejection of small organic molecules was also investigated (Figure 7d). The filtration of aqueous solutions (50 μM) of three molecules of similar size, Riboflavin (Rib, 1.02 nm), Rose Bengal (RB, 1.08 nm), and Rhodamine B (RhB, 1.14 nm), was performed. In all cases, rejection in the *cis* membrane is lower, irrespective of the size of the dyes. The rejection increases again when the membrane is isomerized back to its *trans* state. The change in rejection between the *cis* and the *trans* state is higher for the largest dye (RhB), probably because the pore size of the *trans* state (1.2 nm) is close to the size of this dye (1.14 × 1.63 nm). The smaller dyes, Rib and RB, show a weaker dependence on the isomerization state. Rejection of the neutral dye Rib, especially in the *cis* state, is lower than that of the anionic dye RB as a result of the repulsion between the negatively charged dye RB and the sulfonate groups within the pores, in line with the previously reported work of nonswitchable membranes.[31] The slightly higher transport for the *trans* state after irradiation than the initial *trans* can be attributed to incomplete recovery after irradiation at 455 nm. These observations suggest that the strongest effects of pore size modulation can be expected for molecules such as Rhodamine B. that are close in size to the pore size of the membrane. However, as shown before, the filtration of neutral PEG molecules of different Mn shows larger differences between both isomerization states, which enhances the size photo-switching effect of the system.

3. Conclusions

In this work, a reversible photo-switchable water filtration membrane based on a polymerized liquid crystal is presented. The supramolecular discotic liquid crystal (SulfAzo$_3$TB) containing azo moieties was used as the photo-responsive system. Crosslinking of the columnar network, followed by the removal of the TB template, led to a nanoporous material that was used as the active layer in a filtration membrane. The long lifetime of the *cis* isomer in solid-state (5.7 h) allowed the study of the filtration properties of the membrane in each isomeric state. Reversible changes in water permeability and molecular transport of organic solutes are induced by light, demonstrating that this membrane is a light-controlled separation system. In contrast with other filtration membranes based on liquid crystals, our material offers the possibility to change the transport of solutes in water with light, based on size selectivity that varies for each isomeric state. Other reported photo-switchable systems that also show changes in ion transport and on–off passage of model molecules. However, they have not been applied as water filtration membranes as it is presented here. In this work, we claim the possibility to tailor the rejection of solutes, with even on–off passage situations depending on the molecular size, which brings the potential of this dynamic membrane for its application in selective removal of contaminants or recovery of valuable components.

4. Experimental Section

Film Preparations: Clean glass substrates (3 × 3 cm) were prepared by washing with acetone and isopropanol and finally dried. The nanoporous materials were made by making a solution of 4-((2,3,4-tris(undec-10-en-1-yloxy)phenyl)diazenyl)-benzoic acid 3 (3.2 equivalents) and 1,10-decanedithiol (4.8 equivalents) in CHCl$_3$/MeOH (9:1 v/v) and adding this solution to the required amount of 1,3,5-tris(5-methyl-1H-benzo[d]imidazol-2-yl)benzene (TB, 1 equivalent) (50 mg ml^{-1}). Finally, Bis(2,4,6-trimethylbenzoyl)-phenylphosphineoxide (Irgacure 819, 3 wt%) was added as photo-initiator. One hundred to two hundred microliters of the solution was casted on a clean glass substrate of 3 × 3 cm. The solvent was slowly evaporated in a heating plate at 70 °C and the sample was photo-polymerized using an EXFO Omnicure S2000 lamp with 8 mW cm^{-2} of intensity, for 10 min, resulting in a bright orange nonsoluble polymer. Then, the sample was placed in dimethyl sulfoxide and shacked for 2 h to remove the template. After a washing step with water, the films were dried under a vacuum at 40 °C.

Membrane Fabrication: Glass plates were cleaned with acetone and isopropanol under sonication for 10 min in a bath. Solutions for spin coating were prepared by mixing SulfAzo (3.2 equivalents) with TB (1 equivalent) and 1,10-decanedithiol (4.6 equivalents) in dichloromethane/ethanol (8:2 v/v) in a 10 wt% concentration. Finally, Bis(2,4,6-trimethylbenzoyl)-phenylphosphineoxide (Irgacure 819, 3 wt%) was added as an initiator. A sacrificial layer of polystyrene sulfonate (PSS) was used to avoid de-wetting of the monomer mixture afterward. A 10 wt% aqueous solution was spin-coated on the clean glass at 1500 rpm for 60 s. Then the monomer mixture was spin-coated on top at 2500 rpm for 30 s. The resulting LC/PSS was transferred to a polyethersulfone (PES) support. The "sandwich" was heated to 70 °C and hand-pressed with a steal roller to help the transfer. After further cooling to room temperature, the membrane was polymerized with UV light for 15 min with 8 mW cm^{-2} of intensity, which was provided with a 400 nm cutoff filter (Newport), to avoid the isomerization from *trans* to *cis* of the azobenzene moiety during polymerization. The glass and PSS sacrificial layer were removed by immersing the composite membrane in water and the obtained membrane was dried in a vacuum oven at 40 °C.

**ADVANCED
SCIENCE NEWS**

www.advancedsciencenews.com

**ADVANCED
MATERIALS
INTERFACES**

www.advmatinterfaces.de

UV-Vis Switching Experiments: The photoinitiated switching between trans and cis was measured by making a solution of SulfAzo (13.8 mg) in 0.7 ml of chloroform (100 µM). The UV-Vis spectrum was measured with a baseline set for chloroform. *Trans* to *cis* switching was measured by irradiating with 365 nm UV light (700 mA) for 15 min and measuring a new UV-Vis spectrum after irradiation. *Cis* to *trans* switching was measured by irradiating the *cis* sample for 15 min with blue light of 455 nm (350 mA) and measuring the UV-Vis spectra. The photo-isomerization processes between *trans-cis-trans* of the polymer were measured in solid-state onto glass substrates via UV-Vis spectroscopy. The baseline is set for the clean glass. *Trans* to *cis* switching was measured by irradiating with 365 nm UV light (700 mA) for 1 h to reach the *cis* state. *Cis* to *trans* back switching was measured in the UV-Vis spectra by irradiating the sample for 15 min with the blue light of 455 nm (350 mA). The corresponding *trans-cis-trans* cycles were repeated once to check the behavior repeats

Water Filtration Tests: The permeability of the membranes was determined by measuring the flux of pure water at different pressures (1–5 bar) using a 20 ml custom-made, stainless steel, stirred "Amicon type" dead-end filtration cell of 1.5 cm diameter. Samples of the membrane were cut to the desired size and precleaned with deionized water. For each filtration test, a membrane was placed in the cell which was filled with ultrapure water (total volume of 20 ml) and was pressurized with nitrogen at the maximum pressure of 5 bar for 2 h to stabilize the membrane. Permeate weight was measured in triplo increasing P from 1 to 5 bar. The permeate at each pressure was collected once a steady-state flux was reached and was converted to volume to obtain the water flux, J (L m^{-2} h^{-1}), which was proportional to the pressure difference. Plotting J over ΔP (bar) gave a linear relation from which the permeability **P** (L m^{-2} h^{-1} bar^{-1}) was calculated following:

$$P = \frac{J}{\Delta P}$$

MWCO Determination: Membranes were subjected to polyethylene glycol (PEG) filtrations at 4 bar using the same Amicon cell. Aqueous solutions in ultrapure water were made containing five PEGs with a number of average molecular weights (Mn) ranging from 600 to 10 000 g mol^{-1} with a concentration of 0.5 g L^{-1} for each polymer. 10 ml of two solutions of three different Mn PEG (from 600 to 4000 and from 4600 to 1×10^4 g mol) were filtered separately and 3 fractions of 1 ml of permeate solution were collected. The composition of the feed and the permeate solutions was analyzed by Size Exclusion Chromatography (SEC) in dimethyl formamide. The collected fractions of 1 ml of each permeate sample were evaporated separately and dissolved in 1 ml of DMF. For each analysis, 10 µl of the sample was injected into the SEC, which ran at 10 ml min^{-1}. The concentration of PEG was detected with a photodiode array detector. The corresponding calibration curve is applied to convert the rejection time to molecular weight. The average peaks obtained from each solution were normalized to the injection peak of the measurement.

The rejection (R) was calculated from the difference of the maximum intensity of the peaks of the feed (F) and permeate (P) as:

$$R(\%) = \frac{I_F - I_P}{I_F} \times 100(\%).$$

Pore size values were calculated from the relation between molecular weight and hydrodynamic radius for PEG given by the following equation:[45] $R_h = 0.06127 \cdot Mn^{0.3931}$

Filtration of Neutral and Charged Organic Molecules: Aqueous solutions of the three organic dyes (RB, RhB, and Rib) with molecular weights between 330 and 892 g mol^{-1} were used for filtration tests. The solutions (50 µM) were filtered at 4 bar pressure in the Amicon setup. Once a steady-state was reached, samples of the permeate were collected in triplo to determine the average rejection. Samples were immediately measured in UV-Vis between 300 and 600 nm in a quartz microcuvette. Rejection (R) of each dye was determined by comparing the intensity (I) of the maxima of each dye in UV absorbance of the feed (F) and the permeate (P) solutions: $R(\%) = \frac{I_F - I_P}{I_F} \times 100(\%).$

Statistical Analysis: Filtration experiments were analyzed with the following statistical procedure:

Water permeability was obtained from the average of three values of three different membranes at 4 bar pressure. The rejection values for different Mw PEGs were obtained from the average value of 3 different permeate fractions of three membranes. The standard deviation was calculated as well (Table S3, Supporting Information). The same applies to the rejection of organic dyes (Figure 7c); average and standard deviation of three permeate samples from three membranes.

Supporting Information

Supporting Information is available from the Wiley Online Library or from the author.

Conflict of Interest

The authors declare no conflict of interest.

Data Availability Statement

The data that support the findings of this study are available in the supplementary material of this article.

[1] M. A. C. Stuart, W. T. S. Huck, J. Genzer, M. Müller, C. Ober, M. Stamm, G. B. Sukhorukov, I. Szleifer, V. V. Tsukruk, M. Urban, F. Winnik, S. Zauscher, I. Luzinov, S. Minko, *Nat. Mater.* **2010**, *9*, 101.
[2] F. Ercole, T. P. Davis, R. A. Evans, *Polym. Chem.* **2010**, *1*, 37.
[3] A. Goulet-Hanssens, F. Eisenreich, S. Hecht, *Adv. Mater.* **2020**, *32*, 1905966.
[4] M. Irie, *Photoresponsive Polymers*, Vol. *94*, Elsevier Ltd, Cham, Switzerland **1990**.
[5] J. Henzl, M. Mehlhorn, H. Gawronski, K. H. Rieder, K. Morgenstern, *Angew. Chem., Int. Ed.* **2006**, *45*, 603.
[6] H. M. D. Bandara, S. C. Burdette, *Chem. Soc. Rev.* **2012**, *41*, 1809.
[7] H. Yu, *J. Mater. Chem. C* **2014**, *2*, 3047.
[8] A. H. Gelebart, D. Jan Mulder, M. Varga, A. Konya, G. Vantomme, E. W. Meijer, R. L. B. Selinger, D. J. Broer, *Nature* **2017**, *546*, 632.
[9] D. Xia, G. Yu, J. Li, F. Huang, *Chem. Commun.* **2014**, *50*, 3606.
[10] H. Zhang, W. Tian, R. Suo, Y. Yue, X. Fan, Z. Yang, H. Li, W. Zhang, Y. Bai, *J. Mater. Chem. B* **2015**, *3*, 8528.

[11] A. H. Gelebart, D. Liu, D. J. Mulder, K. H. J. Leunissen, J. van Gerven, A. P. H. J. Schenning, D. J. Broer, *Adv. Funct. Mater.* **2018**, *28*, 1705942.

[12] W. Danowski, T. Van Leeuwen, W. R. Browne, B. L. Feringa, *Nanoscale Adv.* **2021**, *3*, 24.

[13] E. Pantuso, G. De Filpo, F. P. Nicoletta, *Adv. Opt. Mater.* **2019**, *7*, 1900252.

[14] M. Alvaro, M. Benitez, D. Das, H. Garcia, E. Peris, *Chem. Mater.* **2005**, *17*, 4958.

[15] H. P. C. Van Kuringen, Z. J. W. A. Leijten, A. H. Gelebart, D. J. Mulder, G. Portale, D. J. Broer, A. P. H. J. Schenning, *Macromolecules* **2015**, *48*, 4073.

[16] K. Müller, J. Wadhwa, J. Singh Malhi, L. Schöttner, A. Welle, H. Schwartz, D. Hermann, U. Ruschewitz, L. Heinke, *Chem. Commun.* **2017**, *53*, 8070.

[17] J. A. M. Lugger, P. P. Marín San Román, C. C. E. Kroonen, R. P. Sijbesma, *ACS Appl. Mater. Interfaces* **2021**, *13*, 4385.

[18] K. Müller, A. Knebel, F. Zhao, D. Bléger, J. Caro, L. Heinke, *Chem. – Eur. J.* **2017**, *23*, 5434.

[19] A. Knebel, L. Sundermann, A. Mohmeyer, I. Strauß, S. Friebe, P. Behrens, J. Caro, *Chem. Mater.* **2017**, *29*, 3111.

[20] N. Minoura, *Chem. Mater.* **2003**, *15*, 4703.

[21] S. N. Ramanan, N. Shahkaramipour, T. Tran, L. Zhu, S. R. Venna, C. K. Lim, A. Singh, P. N. Prasad, H. Lin, *J. Membr. Sci.* **2018**, *554*, 164.

[22] Z. Wang, A. Knebel, S. Grosjean, D. Wagner, S. Bräse, C. Wöll, J. Caro, L. Heinke, *Nat. Commun.* **2016**, *7*, 13872.

[23] T. Kumeria, J. Yu, M. Alsawat, M. D. Kurkuri, A. Santos, A. D. Abell, D. Losic, *Adv. Mater.* **2015**, *27*, 3019.

[24] H. Q. Liang, Y. Guo, Y. Shi, X. Peng, B. Liang, B. Chen, *Angew. Chem., Int. Ed.* **2020**, *59*, 7732.

[25] P. Li, G. Xie, X. Y. Kong, Z. Zhang, K. Xiao, L. Wen, L. Jiang, *Angew. Chem., Int. Ed.* **2016**, *55*, 15637.

[26] K. Xiao, K. Wu, L. Chen, X. Y. Kong, Y. Zhang, L. Wen, L. Jiang, *Angew. Chem., Int. Ed.* **2018**, *57*, 151.

[27] T. Sata, Y. Shimokawa, K. Matsusaki, *J. Membr. Sci.* **2000**, *171*, 31.

[28] Y. Jiang, L. Heinke, *Langmuir* **2021**, *37*, 2.

[29] S. K. Kumar, J. D. Hong, *Langmuir* **2008**, *24*, 4190.

[30] N. Liu, D. R. Dunphy, P. Atanassov, S. D. Bunge, Z. Chen, G. P. López, T. J. Boyle, C. Jeffrey Brinker, *Nano Lett.* **2004**, *4*, 551.

[31] P. Marín San Román, K. Nijmeijer, R. P. Sijbesma, *J. Membr. Sci.* **2021**, *644*, 120097.

[32] A. Kraft, A. Reichert, R. Kleppinger, *Chem. Commun.* **2000**, *12*, 1015.

[33] Y. Zhang, R. Dong, U. R. Gabinet, R. Poling-skutvik, N. K. Kim, C. Lee, O. Q. Imran, X. Feng, C. O. Osuji, *ACS Nano* **2021**, *15*, 8192.

[34] G. M. Bögels, J. A. M. Lugger, O. J. G. M. Goor, R. P. Sijbesma, *Adv. Funct. Mater.* **2016**, *26*, 8023.

[35] S. Bhattacharjee, J. A. M. Lugger, R. P. Sijbesma, *Chem. Commun.* **2018**, *54*, 9521.

[36] J. A. M. Lugger, R. P. Sijbesma, *ChemistryOpen* **2016**, *5*, 580.

[37] X. Zhu, B. Tartsch, U. Beginn, M. Möller, *Chem., A Eur. J.* **2004**, *10*, 3871.

[38] X. Zhu, U. Beginn, M. Möller, R. I. Gearba, D. V. Anokhin, D. A. Ivanov, *J. Am. Chem. Soc.* **2006**, *128*, 16928.

[39] F. Camerel, G. Ulrich, J. Barberá, R. Ziessel, *Chem., A Eur. J.* **2007**, *13*, 2189.

[40] C. Hoyle, C. Bowman, *Angew. Chem., Int. Ed.* **2010**, *49*, 1540.

[41] C. Decker, K. Moussa, *Die Makromol. Chem.* **1988**, *189*, 2381.

[42] E. Merino, M. Ribagorda, *J. Org. Chem.* **2012**, *8*, 1071.

[43] C. S. Paik, H. Morawetz, *Macromolecules* **1972**, *5*, 171.

[44] G. C. Henk, J. Haitjema, G. L. v. Morgen, Y. Yong Tan, *Macromolecules* **1994**, *27*, 6201.

[45] X. Dong, A. Al-Jumaily, I. C. Escobar, *Membranes (Basel)* **2018**, *8*, 23.